Aqueous Phase Oligomerization of Methyl Vinyl Ketone by Atmospheric Radical Reactions

ARTICLE *in* THE JOURNAL OF PHYSICAL CHEMISTRY C · DECEMBER 2014

Impact Factor: 4.77 · DOI: 10.1021/jp5065598

9 AUTHORS, INCLUDING:

Pascal Renard
Université Blaise Pascal - Clermont-Ferrand II
13 PUBLICATIONS **62** CITATIONS
SEE PROFILE

Bruno Coulomb
Aix-Marseille Université
65 PUBLICATIONS **323** CITATIONS
SEE PROFILE

Etienne Quivet
Aix-Marseille Université
40 PUBLICATIONS **252** CITATIONS
SEE PROFILE

THE JOURNAL OF PHYSICAL CHEMISTRY C

Article

pubs.acs.org/JPCC

Aqueous Phase Oligomerization of Methyl Vinyl Ketone by Atmospheric Radical Reactions

Pascal Renard,[†] Allison E. Reed Harris,[‡] Rebecca J. Rapf,[‡] Sylvain Ravier,[†] Carine Demelas,[†] Bruno Coulomb,[†] Etienne Quivet,[†] Veronica Vaida,[‡] and Anne Monod*[,†]

[†]Aix-Marseille Université, CNRS, LCE FRE 3416, 13331, Marseille, France

[‡]Department of Chemistry and Biochemistry, CIRES, University of Colorado at Boulder, UCB 215, Boulder, Colorado 80309, United States

Supporting Information

ABSTRACT: Aqueous phase oxidation reactions in atmospheric particles can yield high molecular weight products and create secondary organic aerosol (SOA) upon droplet evaporation. Oxidation by hydroxyl radicals to create oligomers in solution that form SOA has been previously investigated; however, mixed organic solutions that can initiate radical chemistry have been largely overlooked. In aqueous solution, pyruvic acid (PA), an α-keto acid found in both the gas and aqueous phases in the atmosphere, photolyzes via a radical mechanism. Here, we use this photochemistry of pyruvic acid to trigger oligomerization of methyl vinyl ketone (MVK), an α,β-unsaturated compound generated by the atmospheric oxidation of isoprene. We closely compare the reaction products and mechanism to a recent work in which the radical oligomerization of MVK initiated by hydroxyl radical is studied in depth. Using mass spectrometry, it is shown that the two reactions create oligomers of similar molecular weights, up to m/z 1200 for initial MVK concentrations of 20 mM. In the MVK and PA photolysis, exploring initial reactant concentrations demonstrates that the same oligomer series are produced regardless of the initial reactant or dissolved oxygen concentrations. However, the size of the oligomers formed increases with increasing initial reactant concentrations, and the oligomerization process is slowed when dissolved oxygen is present. Finally, using a Langmuir trough, that measures the surface tension as a function of liquid surface area, it is shown that these oligomer photoproducts are surface active. These results indicate the importance of mixed organic systems to understanding secondary organic aerosol formation and growth. Consequently, this chemistry may affect gas−particle mass transfer of water and semivolatile aerosol components and, therefore, the way that aerosol interacts with its environment.

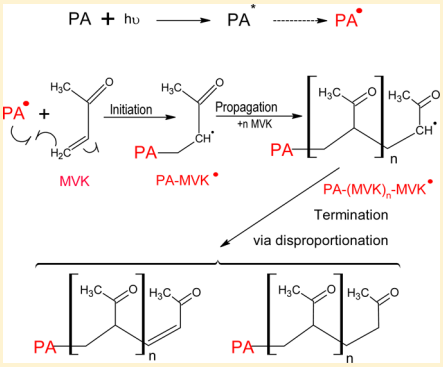

INTRODUCTION

Aerosols play an important role in many atmospheric processes, including cloud nucleation, radiation scattering, and smog evolution, which significantly impact human health and climate.[1−3] Furthermore, quantification of their overall effect on the Earth's radiative budget contributes the largest source of uncertainty in current climate models, motivating fundamental research regarding the chemical and physical properties of aerosols. In addition to inorganic particles, the impact of organic material on aerosol light scattering and cloud initiation has recently been recognized.[4] Globally, only 20% of the organic aerosol mass is emitted directly.[4,5] Therefore, understanding the formation and growth mechanisms for secondary organic aerosol (SOA) is particularly important. SOA production from the gas phase oxidation of volatile organic compounds (VOC) has been extensively studied.[1,4,6] Recently, however, it has become clear that aqueous phase photochemistry, which generates high molecular weight compounds that remain condensed upon water evaporation, is another essential pathway to form SOA.[1,2,7−11] Solution phase processes can be very different from those in the gas phase, thus, aqueous SOA may have unique and characteristic properties.[2,12−15] Additionally, products from these aqueous reactions can partition to the surface of a particle and change its morphology and hygroscopicity, which will in turn affect its lifetime and atmospheric consequences.[16−20]

Isoprene is one important organic compound in the atmosphere, as it comprises about a third of the annual global nonmethane VOC emissions.[21] Methyl vinyl ketone (MVK), an α,β-unsaturated water-soluble organic compound, is among the key oxidative products from isoprene.[22] While the oxidation of isoprene in the gas phase has been linked to the formation of SOA,[23−25] this direct gas-phase SOA formation has not been observed to evolve through an MVK intermediate.[23,25] However, laboratory studies have shown that the aqueous reactivity of some carbonyl compounds, including MVK, creates high molecular weight products that may contribute to SOA formation.[7,8,12,14,26−36] MVK bears highly reactive

Special Issue: John C. Hemminger Festschrift

Received: July 1, 2014
Revised: October 13, 2014

   dx.doi.org/10.1021/jp5065598 | J. Phys. Chem. C XXXX, XXX, XXX−XXX

functional groups (i.e., conjugated carbon−carbon and carbon−oxygen double bonds), which play a major role in the aqueous chemistry that yields these high molecular weight products through (i) acid-catalyzed aldol reactions;[36] (ii) acid-catalyzed hydration followed by oligomerization;[36] and (iii) radical chemistry.[7,35] The aqueous phase reactivity of MVK toward •OH radicals has been studied by several authors.[7,34,35,37] In particular, Renard et al.[7] showed that photooxidation of MVK by •OH in the aqueous phase proceeds via a radical mechanism to create large multifunctional species, or oligomers (polymers consisting of a small number (<30) of repeat units are called oligomers in this context). MVK oxidation by •OH yields initiator radicals, which react with MVK to form oligomers by addition to the vinyl double bond.[7]

In addition to photooxidation initiated by •OH, direct photochemistry of some aldehydes and ketones can be an important tropospheric sink.[35,38] Pyruvic acid (PA), another oxidative product of isoprene, reacts photolytically without •OH in both the gas and the aqueous phases.[13,38−48] Unlike MVK, which has very low quantum yields for photolysis in the solar spectrum, photolysis dominates over the •OH chemistry for PA.[13] The direct aqueous photochemistry of PA proceeds through the excited $^3(n, \pi^*)$ state, which initiates radical chemistry through a hydrogen atom abstraction reaction. This yields reactive radicals that combine to form various products, including dimethyltartaric acid and other oligomers.[13,15,45] Moreover, it has been shown that under certain atmospheric conditions, such as some cloud droplets (liquid water content (LWC) = 0.5 g m^{-3}, pH = 3) or wet aerosols (LWC = 17.6 μg m^{-3}, pH = 1), the aqueous photolysis of PA can be of equal or greater importance to the gas-phase photolysis.[13] Since this reaction increases the molecular weight of compounds in solution, it is important to consider when analyzing aerosol processing.

While the •OH-oxidation of isolated aldehydes or ketones, such as MVK, has been investigated, mixed systems in which photochemically generated radicals other than HO_x trigger oligomerization in solution have been overlooked.[7,15] These reactions, however, are expected to be highly atmospherically relevant, as oxidative products of isoprene are formed simultaneously and likely interact. Because aqueous PA is effective in activating radical chemistry through photolysis under atmospheric actinic flux, the present study investigates the ability of PA to initiate oligomerization of MVK. Here, we show that upon irradiation of a mixed solution of MVK and PA, similar oligomers to the products observed by Renard et al.[7] from the •OH oxidation of MVK, are formed under a range of initial concentrations. These products are significant in at least two ways: (i) this is a new mechanism for creating oligomers in solution that may be atmospherically relevant and (ii) we show here that the products are surface active and may, therefore, change optical properties at air−water interfaces in the environment and potentially contribute to SOA formation.[16−20]

EXPERIMENTAL SECTION

In this work, we used a photoreactor to generate radicals from the photolysis of either pyruvic acid or hydrogen peroxide that then initiate MVK oligomerization reactions. Aqueous aliquots sampled at different photoreaction times were analyzed using liquid chromatography coupled to ultraviolet absorbance spectroscopy (LC-UV) and liquid chromatography coupled to mass spectrometry (LC-MS) in order to quantify the reactants, identify the oligomers produced, and establish a basic mechanism. The products from the reaction initiated by intermediates in the pyruvic acid photolysis were compared to that from the reaction initiated by •OH. Finally, the surface activity of all products was investigated using a Langmuir trough equipped with a Wilhelmy balance.

Photochemical Reaction and Conditions. Described in Renard et al.,[7] a 450 cm^3 stirred Pyrex thermostated photoreactor was equipped with a 1000 W xenon arc lamp (LSB 551, Lot Oriel) and a glass filter, air mass 0 (LSZ 185, Lot Oriel). Photochemical reactions for the surface activity analysis were performed using a similar setup (described by Reed Harris et al.[13]) with a 450 W xenon arc lamp (Newport) and a pyrex lens used to filter radiation below 300 nm.

Reactive radicals to initiate oligomerization were prepared by irradiation of Ultra High Quality (UHQ) water (18.2 Mohm cm, Millipore) with H_2O_2 (50%, stabilized, Sigma-Aldrich) or pyruvic acid (98%, Sigma-Aldrich) for 10 min. MVK (99%, Sigma-Aldrich) was then introduced to begin the reaction and photolysis of the mixture continued for a duration of 300 min. Renard et al.[7] showed that a change in temperature affects only the kinetics of the reaction of MVK with •OH, and not the reaction products. Therefore, in this work, all experiments were performed at 25 °C. Solutions were unbuffered and dissolved oxygen concentrations were not constrained. The temperature, pH, and dissolved oxygen concentrations were continuously monitored in the reaction solution using a Consort C3020 multiparameter analyzer.

Tan et al.[30] have shown the important impact of initial concentrations on oligomer formation for α-dicarbonyls. The PA experiments were therefore carried out at three different initial MVK concentrations, 0.2, 2, and 20 mM, which are comparable to the total concentrations of unsaturated water-soluble organic compound in wet aerosol.[7,49,50] The initial pyruvic acid concentrations (4, 10, and 100 mM, respectively) were also chosen to be consistent with observed amounts of pyruvic acid in the particulate phase in the atmosphere.[51] For the •OH experiments, we used the same highest initial concentration of MVK (20 mM) as in Renard et al.[7] The estimation of the resulting •OH concentrations in these studies (10^{-15} to 10^{-14} M) were close to estimated values for cloud and fog droplets.[52−54]

A solution of pyruvic acid with MVK under dark conditions was monitored by LC-UV for the same duration as the photochemical experiments. Neither was significantly consumed, indicating that no substantial reaction between them occurs without irradiation. Additionally, the direct photolysis of PA (100 mM), in the absence of MVK, as seen in Reed Harris et al.,[13] yielded much shorter oligomers than is observed for the photolysis of the mixed solution of pyruvic acid with MVK. These control experiments ensure that the observed oligomerization is initiated by MVK reaction with •OH or intermediates in the PA photolysis.

Reactants and Products Analysis. *LC-MS Analyses.* Aliquots of the solution sampled from the photoreactor were analyzed for organic species using an ultrahigh performance liquid chromatographic (UPLC) system coupled to a time-of-flight mass spectrometer equipped with an electrospray ionization (ESI) source and an ion mobility cell (Synapt-G2 HDMS, Waters). The resolution of the mass spectrometer (18000 at m/z 400) allowed determination of the chemical formula of the oligomer series. Data were collected from m/z 50 to 1200 in both ionization modes. The chromatographic

dx.doi.org/10.1021/jp5065598 | J. Phys. Chem. C XXXX, XXX, XXX−XXX

separations are carried out on an UPLC column (HSS T3 C18, 2.1 × 100 mm to 1.8 μm; Waters) at 40 °C. The mobile phases consist in (A) 0.1% formic acid in water (Biosolve, 99%) and (B) acetonitrile (Biosolve, ULC/MS). The gradient elution is performed at a flow rate of 600 μL min^{-1} using 5−95% of B within 7 min and held at 95% of B for 1.5 min.

LC-UV Analyses. An UPLC system (Accela 600 auto sampler, Accela 600 pump, Thermo Scientific) coupled to a diode array detector (Accela 600 PDA detector; Thermo Scientific) was used to monitor the concentrations of MVK and PA sampled from the photoreactor. The LC separation was performed using a Hypersil GOLD column (100 × 2.1 mm to 1.9 μm, Thermo Scientific) at 40 °C and at a flow rate of 300 μL min^{-1}. The mobile phase was water/acetonitrile (98:2) (v/v) and the injection volume was set to 2 μL. The spectra were recorded from 200 to 360 nm.

Both PA and MVK show an intense absorption band (K-band; $\pi \rightarrow \pi^*$ transition) in aqueous solution that peaks at 205 and 211 nm, respectively, and a weak absorption band (R-band; $n \rightarrow \pi^*$ transition) that peaks at 319 and 308 nm, respectively. Pyruvic acid has a retention time of 0.5 min and MVK has a retention time of 1.8 min. The absorption intensity at 211 and 229 nm were found to be directly proportional to both the PA and the MVK concentrations over the ranges studied. MVK oxidation by pyruvic acid photolysis was followed by monitoring at 211 nm for the lowest concentrations ($[PA]_0$ = 4 mM and $[MVK]_0$ = 0.2 mM) and at 229 nm for higher concentrations ($[PA]_0$ = 10 and 100 mM and $[MVK]_0$ = 2 and 20 mM).

IC-MS Analyses. Quantification of organic acids in the solutions was performed with an ion chromatography system (Dionex ICS3000) driven by Chromeleon software (version 6.80); composed of a SP-5 gradient pump, an AS40 autosampler, a CD25 conductivity detector; and coupled to a Thermo Scientific Surveyor MSQ (Thermo Electron, U.S.A.) mass spectrometer operated in the ESI negative mode. A 4 mm ASRS 300 electrolytic suppressor operated in external water mode (7 mL min^{-1}) was placed before the conductivity cell. An additional peristaltic pump was used to wash the entrance cone of the mass spectrometer with water at a flow rate of 0.4 mL min^{-1} during measurements. The chromatographic separations were carried out on an IonPac AS11-HC column 4 × 250 mm (Dionex) coupled to a guard column (Dionex AG11-HC, 4 × 50 mm). Samples were injected automatically using a 25 μL loop injection valve. The analysis was performed at 35 °C with a flow rate set at 0.8 mL min^{-1}. Eluent A (UHQ water) and eluent B (100 mM NaOH) were flushed with purified helium gas for 30 min and kept under a nitrogen atmosphere during the procedure. Separation was carried out using an eluent gradient, as follows (min, B %): 0, 1%; 12, 5%; 30, 19%; 40, 40%. The analytes were monitored using the selected ion-monitoring (SIM) mode, and signal areas (counts/min) of each peak were used for quantification.

Surface Activity Studies. The surface activity of solutions both before and after photolysis was determined using a Langmuir trough equipped with a Wilhelmy balance (KSV-NIMA, Biolin Scientific). The custom-built PTFE Langmuir trough (52 × 7 × 0.5 cm) described previously has computer-controlled mechanical barriers, which allow for control of surface area (A).[55] In the experiments presented here, the barriers were opened to a maximum of 300 cm^2 and closed to a minimum area of 30 cm^2 with a constant barrier speed of 75 cm^2 min^{-1}. The trough was filled with ∼200 mL of the solution of interest while the barriers were fully opened, and the system was equilibrated for 1 h before compression to allow the surface-active species to partition to the surface.

The Wilhelmy balance measures surface pressure (π), the difference in surface tension between the solution of interest (γ), and that of pure water (γ_0).

$$\pi = \gamma_0 - \gamma$$

By measuring surface pressure as a function of surface area, surface pressure−area ($\pi - A$) isotherms are obtained, which allow for an understanding of surface thermodynamics of the system.[56] Here, such isotherms are used as a measure of the extent of preferential surface partitioning of molecules based on their hydrophobicity. The more hydrophobic a molecule, the more it partitions to the surface, which disrupts the normal surface tension of water and increases surface pressure. A system with increased surface pressure is indicative of its greater surface activity.

RESULTS AND DISCUSSION

Photoreaction Products of MVK Oxidation by PA. In aqueous solution, pyruvic acid (PA) hydrates to its geminal diol, 2,2-dihydroxypropanoic acid (∼60%).[15,57] Photolysis of unhydrated PA begins with excitation to $^1(n, \pi^*)$, followed by intersystem crossing and internal conversion to $^3(n, \pi^*)$. PA in the triplet exited state (PA*) then abstracts a hydrogen atom from 2,2-dihydroxypropanoic acid, inducing decarboxylation and creation of two radicals, $CH_3C^{\bullet}(OH)C(O)OH$ (alpha lactyl radical, or $PA^{\bullet}$) and $CH_3C^{\bullet}(OH)_2$ (hydrated acetyl radical, or $AA^{\bullet}$). Recombinations of these radicals yield small oligomers, including dimethyltartaric acid (a major product), and acetoin, lactic acid, and acetic acid (minor products).[13,15] In this study, we aim to form high molecular weight compounds from MVK radical chemistry initiated by intermediates in the pyruvic acid photolysis, namely $PA^{\bullet}$, $AA^{\bullet}$, or PA*. (All three intermediates, $PA^{\bullet}$, $AA^{\bullet}$, and PA*, may initiate radical chemistry, but for simplicity, in the text we refer to these initiator radicals using $PA^{\bullet}$ as our example.) The mechanism proposed here is similar to MVK photooxidation by $^{\bullet}OH$, with the new observation that organic radicals, such as those created by PA photolysis, can also start radical oligomerization chemistry.

The aqueous phase oligomerization of MVK initiated by photolysis of pyruvic acid leads to the formation of several series of oligomers similar to the observed products from the MVK $^{\bullet}OH$-oxidation reaction in Renard et al.[7] Figure 1 shows a comparison of combined LC-MS spectra (retention time range: 0−4 min), between MVK PA-photolysis ($[MVK]_0$ = 20 mM, $[PA]_0$ = 100 mM) and MVK $^{\bullet}OH$-oxidation ($[MVK]_0$ = 20 mM, $[H_2O_2]_0$ = 400 mM). In both experiments, oligomer series are clearly visible, with regular spacing of 70.042 amu, which corresponds to the exact mass of MVK. Both systems extend up to m/z 1200, corresponding to 17 monomer units.

Table 1 lists the oligomer series identified by LC-MS in both modes from MVK PA-photolysis (Figure 1). Identification is performed, as in Renard et al.,[7] on the most intense series, which were further confirmed by MS/MS analyses. Some of the oligomer series (S138, S140, and S156) are similar to those described in Renard et al.[7] and can be explained by a common mechanism, that is, H-abstraction from MVK. Other series, including S158, S160, S200, S202, S218, and S220, are specific to the PA-photolysis. In particular, S158 and S160 correspond

dx.doi.org/10.1021/jp5065598 | J. Phys. Chem. C XXXX, XXX, XXX−XXX

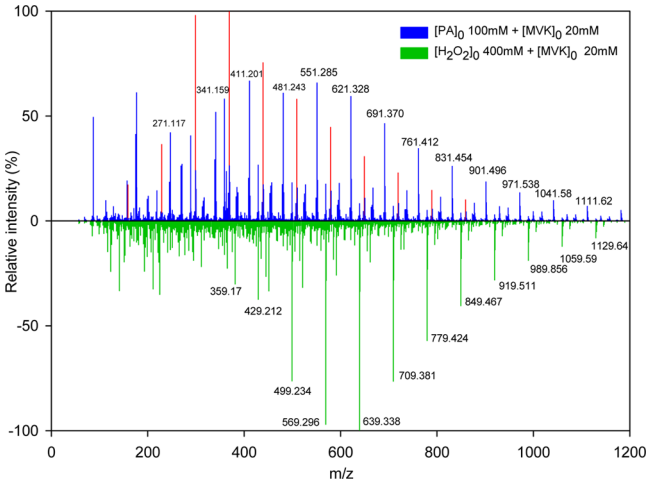

Figure 1. Combined mass spectra for MVK PA-photolysis (blue, $[MVK]_0$ = 20 mM, $[PA]_0$ = 100 mM) and MVK •OH-oxidation (green, $[MVK]_0$ = 20 mM, $[H_2O_2]_0$ = 400 mM) at reaction time of 50 min, obtained using LC-MS for the retention time range 0 to 4 min, in the negative mode. Series S160 (PA-$(MVK)_n$, see Table 1) is highlighted in red.

Table 1. Oligomer Series from MVK PA-Photolysis Identified by LC-MS[a]

oligomer series		detected ions	
name[b]	formulas	formulas[c]	m/z[c]
S138	MVK-$(MVK)_n$	$[C_8H_{10}O_2, +H]^+$	139.0759
S140		$[C_8H_{12}O_2, +H]^+$	141.0916
S156	MVK−OH-$(MVK)_n$	$[C_8H_{12}O_3, +Na]^+$	179.0684
S158	PA-$(MVK)_n$	$[C_7H_{10}O_4, -H]^-$	157.0501
S160		$[C_7H_{12}O_4, -H]^-$	159.0657
S200	$C_5H_8O_4$-$(MVK)_n$	$[C_9H_{12}O_5, -H]^-$	199.0606
S202		$[C_9H_{14}O_5, -H]^-$	201.0763
S218	$C_4H_6O_6$-$(MVK)_n$	$[C_8H_{10}O_7, -H]^-$	217.0348
S220		$[C_8H_{12}O_7, -H]^-$	219.0505

[a]All products were detected as their protonated molecules ($[M + H]^+$) or sodium adducts ($[M + Na]^+$) in the positive mode, and their deprotonated molecules ($[M - H]^-$) in the negative mode. [b]For each series, the name is given by "S" followed by a number corresponding to the nominal mass of the smallest oligomer of the series, i.e., $(MVK)_{n=1}$. [c]Formula and m/z of ions corresponding to the smallest oligomer of each series.

to PA•-addition to MVK, as illustrated in Figure 2, and discussed further below.

In this work, we also detected by IC-MS (Figure S1) low molecular weight reaction products in addition to larger oligomers. Acetic, oxalic, and succinic acids were produced during the reaction of MVK with both PA• and •OH as radical initiators. The presence of common acids regardless of radical initiator is a further indication of the similarity of the oligomerization mechanisms. Lactic acid, however, was observed during photolysis of PA with MVK but not during MVK •OH-oxidation. Lactic acid is also seen in the photolysis of pyruvic acid alone, formed by H-abstraction from AA• by PA•.[13,15,58] The presence of lactic acid in the mixed solution of MVK and PA, therefore, is likely due to this PA• chemistry rather than some difference in oligomerization mechanism due to the specific initiator radical.

Based on the mechanism for MVK radical oligomerization initiated by •OH-oxidation detailed in Renard et al.,[7] we

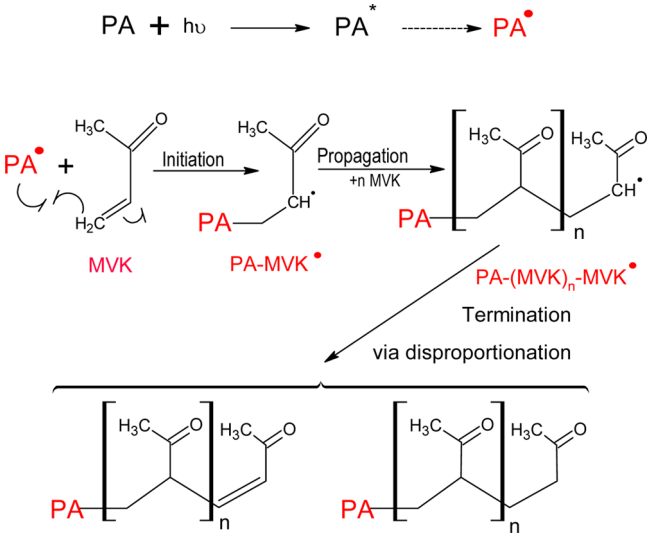

Figure 2. Proposed mechanism of radical oligomerization of PA-$(MVK)_n$ series (S158 and S160) in the aqueous phase, initiated by PA-photolysis. PA• is an initiator radical; MVK is the monomer, n is the degree of oligomerization, that is, chain length. For clarity, only the external radical additions are shown.

propose a similar process for oligomerization of MVK initiated by PA• (Figure 2) to explain the formation of oligomer series S158 and S160 (Table 1). The reaction proceeds primarily as proposed by Renard et al.:[7] oligomerization begins when PA• opens the vinyl double bond of MVK and forms another radical (PA-MVK•) that continues to add MVK monomer units until radical termination. Termination occurs by bimolecular reaction between two radicals, via either recombination or disproportionation. This yields two oligomer series, one saturated and one unsaturated terminal group.[59] For clarity, Figure 2 depicts only reactions in which PA• adds to the β-carbon of MVK, as this is favored over addition to the α-carbon.[7,60] However, either reaction is possible with PA*, AA•, or PA•, leading to a number of isomers that grow exponentially with oligomer chain length.

This chemical mechanism is justified by three experimental observations: (i) the regular mass spacing of 70.042 amu observed in mass spectra (Figure 1) corresponds exactly to the mass of the monomeric MVK; (ii) the faster consumption of MVK compared to that of pyruvic acid (19 mM of MVK is consumed within 95 min while 12 mM of PA is consumed within this time) (Figure 3); and (iii) the strong dependence of oligomer chain length on initial MVK concentration (see next section).

Effect of Reaction Conditions on MVK Oligomerization. In this study, we observe MVK oligomerization under a variety of initial reactant and dissolved oxygen concentrations. Specifically, the reaction was performed at three different initial MVK concentrations: 20 mM ($[PA]_0$ = 100 mM), 2 mM ($[PA]_0$ = 10 mM), and 0.2 mM ($[PA]_0$ = 4 mM), and the results compared.

First, we provide a brief comment on the effect of the radical initiator (PA• vs •OH) on the kinetics of MVK oligomerization to illustrate the role of dissolved oxygen. The observed kinetics of MVK degradation by PA-photolysis are distinct from those performed through •OH-oxidation and dependent on initial PA concentrations (Figures 3 and S2). This contrast may be due to different concentrations of dissolved O_2 between the systems,

dx.doi.org/10.1021/jp5065598 | J. Phys. Chem. C XXXX, XXX, XXX−XXX

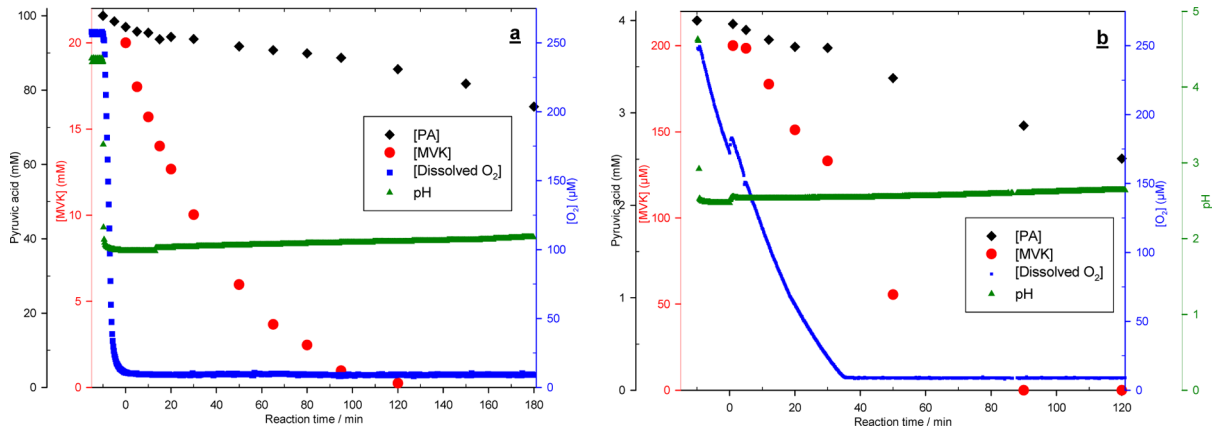

Figure 3. Time profile of the concentrations of PA, MVK, and dissolved O_2, as well as pH during MVK PA-photolysis (a) for high initial precursor concentrations ($[MVK]_0$ = 20 mM, $[PA]_0$ = 100 mM); (b) for very low initial precursor concentrations ($[MVK]_0$ = 0.2 mM, $[PA]_0$ = 4 mM). Data were recorded beginning at reaction time, t = −15 min, with introduction of PA at t = −10 min and MVK at t = 0 min.

as O_2 is known to slow free radical photo-oligomerization.[61] The slowed kinetics is caused by O_2 quenching the excited state of the photoinitiator and by fast O_2 addition on primary initiating and propagating radicals. This yields peroxyl radicals ($RO_2^{\bullet}$), which are moderately reactive and can terminate propagation or may even initiate slow reactions of polymerization in specific cases.[62,63] Under our $^{\bullet}$OH-oxidation of MVK experimental conditions, photolysis of H_2O_2 induces supersaturated oxygen conditions prior to MVK introduction (mechanism shown in Table S1).[7] The result is a slow initial decay of MVK (Figure S2) relative to the remainder of the reaction. Conversely, in the MVK with PA-photolysis experiments, conducted at high initial concentrations, the photolysis of 100 mM PA consumes most of the dissolved oxygen present (decreasing from 258 to 12 μM) during the 10 min of photolysis prior to addition of MVK (Figure 3a). Therefore, oligomerization occurs quickly upon addition of MVK, inducing a faster initial decay of MVK than in the $^{\bullet}$OH-oxidation experiments (Figure S2).

Due to the tendency of PA*, PA$^{\bullet}$, and AA$^{\bullet}$ to consume O_2 under high initial concentrations of photoinitiators, the experiment presented above (Figure 1) was performed under depleted dissolved oxygen concentrations ($[O_2] \leq 12$ μM, Figure 3a). To test for oligomerization under more relevant atmospheric conditions, we explored the influence of the presence of dissolved O_2 on product formation using low initial precursor concentrations ($[MVK]_0$ = 0.2 mM and $[PA]_0$ = 4 mM, compared with $[MVK]_0$ = 20 mM and $[PA]_0$ = 100 mM in Figure 1) (Figures 3 and S3). Because of the lower pyruvic acid concentration, this investigation shows a much slower depletion in dissolved O_2 before MVK is added, causing substantial amounts of O_2 to be present in the solution during the MVK and PA reaction. Under these conditions, molecular weight compounds up to m/z 300, including some oligomers, are observed (as compared with m/z 1200 in Figure 1). Although oxygen reactivity toward PA$^{\bullet}$ is by far the dominating process under these conditions,[13] PA addition to MVK is still competitive. The oligomer series (S160) PA-$(MVK)_n$ is detected under these conditions (for n = 1, and a very weak signal for n = 2) at t = 5 min of reaction (Figure S3), when $[O_2]$ = 160 μM (Figure 3b). This result shows that the initiation reaction by PA$^{\bullet}$ on MVK (Figure 2) remains active under more atmospherically relevant amounts of dissolved oxygen.

The smaller oligomers observed in the low concentration conditions above may be due both to the presence of oxygen acting as a radical quencher as well as the low concentrations used. Initial concentrations of photooxidation precursors are known to influence the kinetics of oligomerization and the size of resulting oligomers.[7,62] We explored these issues by comparing reactions with initial MVK concentrations of 20 mM ($[PA]_0$ = 100 mM) and 2 mM ($[PA]_0$ = 10 mM). Both of these reactions were depleted in dissolved oxygen ($[O_2] \leq 12$ μM) when MVK was added, and thus, the kinetic and product differences can be attributed solely to reactant concentrations. The lower the concentrations, the faster the oligomers reached the maximum of LC-MS relative intensity. For example, while this peak in oligomer intensity was reached after 50 min for 20 mM MVK, it was reached in 15 min for 2 mM MVK. Figure 4 compares the mass spectra for these two reactions at their peak in oligomer intensity (50 and 15 min, respectively).

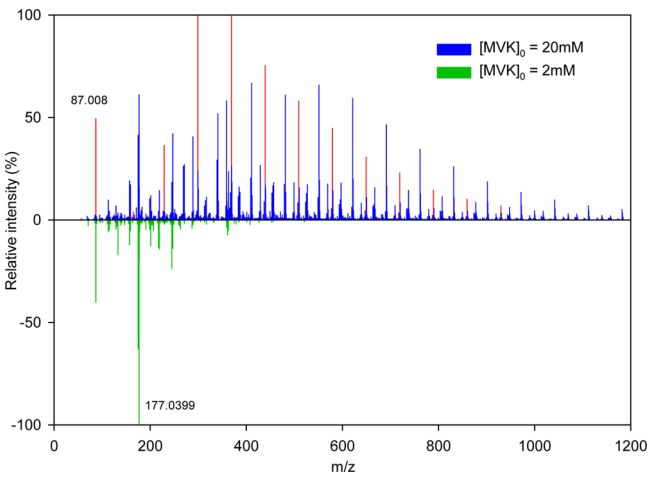

Figure 4. Combined mass spectra of the peak relative oligomer intensity of the MVK PA-photolysis at two different initial reactant concentrations, higher (blue, $[MVK]_0$ = 20 mM, $[PA]_0$ = 100 mM, t = 50 min) and lower (green, $[MVK]_0$ = 2 mM, $[PA]_0$ = 10 mM, t = 15 min), obtained using LC-MS for the retention time range 0 to 4 min, in the negative mode. The peak labeled at m/z 87.008 corresponds to pyruvic acid; the peak labeled at m/z 177.0399 corresponds to the recombination of PA$^{\bullet}$ + PA$^{\bullet}$, dimethyltartaric acid. In the top panel, PA and Series S160 (PA-$(MVK)_n$, see Table 1) is highlighted in red.

dx.doi.org/10.1021/jp5065598 | J. Phys. Chem. C XXXX, XXX, XXX−XXX

Upon inspection of these mass spectra, it is clear the initial concentrations of MVK and PA also strongly affected the extent of oligomerization (Figure 4). In both experiments, the same major series of oligomers were observed, but chain lengths increased with increasing initial MVK concentration. At the lower initial concentration of MVK (2 mM), oligomers up to m/z 400 are formed, and the recombination of radicals becomes important as compared to addition to MVK. The most intense peak (m/z 177.04) in the 2 mM MVK reaction (Figure 4) corresponds to the recombination of two PA$^{\bullet}$ to make dimethyltartaric acid. Conversely, the higher initial concentration of MVK (20 mM) allows for more propagation and thus longer chain lengths, resulting in the formation of high molecular weight reaction products up to m/z 1200 (Figure 4).

The combined results from the three different initial reactant concentrations demonstrates that the same oligomer series are produced in the MVK and PA photolysis regardless of the initial reactant or dissolved oxygen concentrations. However, the size of the oligomers formed increases with increasing initial reactant concentrations and decreasing concentrations of dissolved oxygen.

Surface Activity of Reaction Photoproducts. π–A isotherms taken of a monolayer of a single surfactant yield quantitative thermodynamic information about the behavior and ordering of the surfactant at the surface of an aqueous solution.[53] Specifically, the molecular footprint of the surfactant is obtained. The difficulty of extracting quantitative values increases as the system complexity increases. Monitoring the preferential partitioning of soluble molecules to the surface from a bulk solution presents experimental and conceptual challenges in obtaining numerical results. In this study, π–A isotherms were taken of mixtures of molecules, including postphotolysis products, in a bulk solution, making quantitative speciation and analysis untenable. This complexity does not, however, preclude making very useful, qualitative comparisons between reagents, products, and different reaction systems.

The postphotolysis solutions containing the photooxidation products of MVK (at 20 mM) clearly show increased surface partitioning compared to the prephotolysis controls, regardless of precursors (see Figure 5).

For both control experiments (MVK + H_2O_2 and MVK + PA, no irradiation), the prephotolysis solutions show little surface activity, with only minor increases in surface pressure at low surface areas. This is a further confirmation that very little oligomerization of MVK occurs without photochemical radical initiation. In contrast, the postphotolysis oxidation products of MVK show very significant partitioning to the surface, indicating that the oligomers formed during photolysis have considerable surface activity. Qualitatively, the postphotolysis products appear to have close to the same degree of surface activity using either $^{\bullet}$OH-oxidation or PA-photolysis. This is another indication that a similar degree of oligomerization of MVK occurs for initiation with either $^{\bullet}$OH or PA$^{\bullet}$ radicals. Additionally, at the higher initial MVK and PA concentrations (20 mM and 100 mM, respectively), the postphotolysis solution shows a larger increase in surface pressure than for the less concentrated solution (Figure 5), which is consistent with the higher concentration of longer-chained oligomers formed under these conditions and observed by LC-MS analysis.

Atmospheric Implications. It is increasingly recognized that aqueous phase photooxidation reactions initiated by $^{\bullet}$OH radicals can create high molecular weight oligomers in atmospheric particles. When water evaporates, these oligomers likely remain in the particulate phase, thus increasing SOA mass.[10,11,35] The results obtained in this study suggest that similar reactions can be triggered by organic radicals in solution, demonstrating a new mechanism by which SOA can be created. In this work, we show that MVK, an unsaturated, water-soluble organic compound, produces oligomers of similar mass via both $^{\bullet}$OH-oxidation and PA-photolysis.

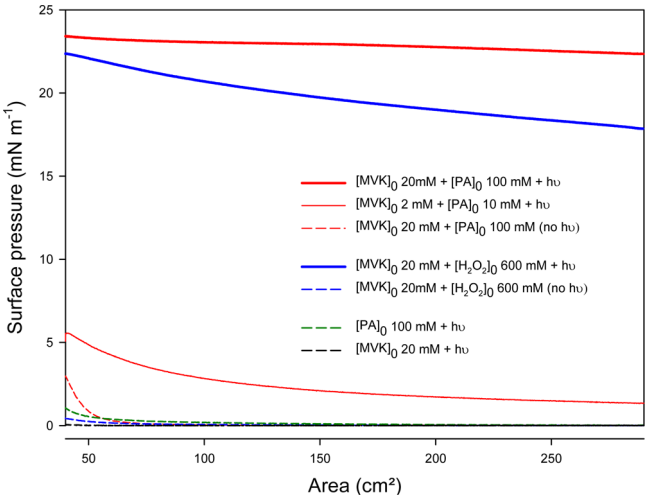

Figure 5. Surface pressure–area isotherms for aqueous phase oligomerization of methyl vinyl ketone by radical reactions and control experiments. Dashed lines correspond to control experiments, which show very little surface activity compared to the radical oligomerization reaction products shown in solid ($[MVK]_0$ = 20 mM) and thin ($[MVK]_0$ = 2 mM) lines. The initial concentration of H_2O_2 was increased to 600 mM for the surface activity studies in order to compensate for the decrease in reaction kinetics associated with the 450 W lamp compared to the 1000 W lamp.

The experimental conditions investigated in this study indicate that, under depleted concentrations of dissolved oxygen ($\leq$12 μM), initial reactant concentrations greatly affect the oligomer chain length, with a chain length decrease by a factor of 3 when initial concentrations of MVK and PA are decreased by an order of magnitude. Using even lower initial precursor concentrations results in much slower depletion of dissolved oxygen concentrations and shows that the initiation reaction of pyruvic acid excited triplet state (PA*) and PA$^{\bullet}$ radical on MVK remains active under the presence of more atmospherically relevant amounts of unsaturated water-soluble organic compounds and dissolved oxygen ($[O_2]$ = 160 μM). The mechanisms for O_2 inhibition on photopolymerization have been extensively investigated, focusing on industrial applications for the production of long chain polymers ($m/z \geq 10000$),[63] but extremely limited studies have investigated this complex chemistry under environmental conditions for the formation of oligomers with $m/z < 2000$.[7,50,64] More studies are thus needed to investigate the likely different precursors and oligomer chain lengths of atmospheric relevance.

Furthermore, it is interesting to compare the efficiency of the initiation steps between MVK $^{\bullet}$OH-oxidation and MVK PA-photolysis. A simple estimate (Table S2) shows that under atmospheric conditions where aqueous concentrations of $^{\bullet}$OH radicals are limited and where pyruvic acid is highly concentrated, such as in wet aerosols,[51,60] the initiation steps between MVK $^{\bullet}$OH-oxidation and MVK PA-photolysis can be of the same order of magnitude. This estimation emphasizes

dx.doi.org/10.1021/jp5065598 | J. Phys. Chem. C XXXX, XXX, XXX–XXX

the relevance of studying radical oligomerization initiated by radicals other than •OH and especially those arising from the photolysis of atmospheric organic compounds.

The resulting products from both reactions are surface active, indicating that these oligomers partition preferentially to an air−water interface, such as the surface of an aerosol. This partitioning could facilitate oligomerization by increasing the concentration of radicals at the surface and may lead to SOA formation or a change in the atmospheric processing of the particle. This is a new mechanism for the formation of organic oligomers, as well as a demonstration of the surface partitioning of the resultant high molecular weight compounds. Surface organic coatings have long been proposed to exist on atmospheric aerosols providing hydrophobic enclosures that, upon aging, can be oxidized in the atmosphere to acquire hydrophilic sites.[18,65,66] As field measurements of atmospheric particles provided molecular speciation, it was confirmed that surface active organics are important components in atmospheric particles with consequences to their optical and chemical properties and overall effect on climate.[19,20,67−75]

Organic surface films can also provide barriers to transport across the air−particle interface, inhibiting uptake of gas phase species.[76−81] These organic films can be an auspicious medium for solubilizing gas phase organic species which may perhaps explain the observed non-Henry's law concentration of organics in field samples.[82] Organic surfactant films provide a special reaction environment, which affects heterogeneous atmospheric chemistry, changing the hygroscopic properties of organically coated particles during their atmospheric lifetime.[19,83−91] Organic films may affect the morphological, optical, and chemical properties of atmospheric aerosols, having potentially important consequences to the direct and indirect effects on the Earth's climate.[92] The results presented here highlight a new, atmospherically plausible, way to create surface active oligomers, which may play a role in the aerosol processing and surface chemistry of the atmosphere.

■ ASSOCIATED CONTENT

Supporting Information

A full description of IC-MS analyses, a comparison of the decay of MVK when oligomerization is induced with •OH vs •PA, a mass spectrum from the lowest initial concentration of the MVK and PA reaction (demonstrating oligomerization initiation step with oxygen present), a mechanism for the formation of O_2 from photolysis of H_2O_2 in our experimental setup, and calculations to compare the initiation rates between MVK •OH-oxidation and the MVK and PA photolysis reactions. This material is available free of charge via the Internet at http://pubs.acs.org.

■ AUTHOR INFORMATION

Corresponding Author

*E-mail: anne.monod@univ-amu.fr.

Notes

The authors declare no competing financial interest.

■ ACKNOWLEDGMENTS

We thank the French National Research Agency ANR (Project CUMULUS ANR-2010-BLAN-617-01), AXA insurances, CIRES fellowship, and CNRS-INSU for funding this research. We thank Assia Smaani (Aix-Marseille university) for contributing to the experimental work on MVK PA-photolysis experiments under high precursor concentrations. We also thank Barbara Ervens (CIRES, University of Colorado, Boulder and Chemical Sciences Division, National Oceanic and Atmospheric Administration (NOAA), Boulder, CO, U.S.A.) for useful discussions and Elizabeth C. Griffith for the suggestion to perform this experiment (CIRES and Department of Chemistry and Biochemistry, University of Colorado, Boulder). V.V., R.J.R., and A.E.R.H. gratefully acknowledge financial support from the National Science Foundation (CHE 1306386). This work was supported by NASA Headquarters under the NASA Earth and Space Science Fellowship Program - Grant NNX13AP85H for R.J.R. This material is based upon work supported by the National Science Foundation Graduate Research Fellowship for AERH under Grant No. (DGE 1144083). Any opinion, findings, and conclusions or recommendations expressed in this material are those of the authors(s) and do not necessarily reflect the views of the National Science Foundation.

■ REFERENCES

(1) Hallquist, M.; Wenger, J. C.; Baltensperger, U.; Rudich, Y.; Simpson, D.; Claeys, M.; Dommen, J.; Donahue, N. M.; George, C.; Goldstein, A. H.; et al. The Formation, Properties and Impact of Secondary Organic Aerosol: Current and Emerging Issues. *Atmos. Chem. Phys.* **2009**, *14*, 5155−5236.

(2) George, C.; D'Anna, B.; Herrmann, H.; Weller, C.; Vaida, V.; Donaldson, D. J.; Bartels-Rausch, T.; Ammann, M. Emerging Areas in Atmospheric Photochemistry. *Atmospheric and Aerosol Chemistry*, Book Series: Topics in Current Chemistry; McNeill, V. F., Ariya, P. A., Eds.; Springer: New York, **2014**, *339*, 1−53.

(3) Ervens, B.; Turpin, B. J.; Weber, R. J. Secondary Organic Aerosol Formation in Cloud Droplets and Aqueous Particles (aqSOA): A Review of Laboratory, Field and Model Studies. *Atmos. Chem. Phys.* **2011**, *11*, 11069−11102.

(4) Kanakidou, M.; Seinfeld, J. H.; Pandis, S. N.; Barnes, I.; Dentener, F. J.; Facchini, M. C.; Van Dingenen, R.; Ervens, B.; Nenes, A.; Nielsen, C. J.; et al. Organic Aerosol and Global Climate Modelling: A Review. *Atmos. Chem. Phys.* **2005**, *5*, 1053−1123.

(5) Spracklen, D. V.; Jimenez, J. L.; Carslaw, K. S.; Worsnop, D. R.; Evans, M. J.; Mann, G. W.; Zhang, Q.; Canagaratna, M. R.; Allan, J.; Coe, H.; et al. Aerosol Mass Spectrometer Constraint on the Global Secondary Organic Aerosol Budget. *Atmos. Chem. Phys.* **2011**, *11*, 12109−12136.

(6) Kroll, J. H.; Seinfeld, J. H. Chemistry of Secondary Organic Aerosol: Formation and Evolution of Low-Volatility Organics in the Atmosphere. *Atmos. Environ.* **2008**, *42*, 3593−3624.

(7) Renard, P.; Siekmann, F.; Gandolfo, A.; Socorro, J.; Salque, G.; Ravier, S.; Quivet, E.; Clément, J. L.; Traikia, M.; Delort, A. M.; Voisin, D.; et al. Radical Mechanisms of Methyl Vinyl Ketone Oligomerization through Aqueous Phase OH-Oxidation: on the Paradoxical Role of Dissolved Molecular Oxygen. *Atmos. Chem. Phys.* **2013**, *13*, 6473−6491.

(8) Carlton, A. G.; Wiedinmyer, C.; Kroll, J. H. A Review of Secondary Organic Aerosol (SOA) Formation from Isoprene. *Atmos. Chem. Phys.* **2009**, *9*, 4987−5005.

(9) Volkamer, R.; SanMartini, F.; Molina, L. T.; Salcedo, D.; Jimenez, J.; Molina, M. J. A Missing Sink for Gas-Phase Glyoxal in Mexico City: Formation of Secondary Organic Aerosol. *Geophys. Res. Lett.* **2007**, *34*, L19807.

(10) Loeffler, K. W.; Koehler, C. A.; Paul, N. M.; De Haan, D. O. Oligomer Formation in Evaporating Aqueous Glyoxal and Methyl Glyoxal Solutions. *Environ. Sci. Technol.* **2006**, *40*, 6318−6323.

(11) Carlton, A. G.; Turpin, B. J.; Lim, H.; Altieri, K. E.; Seitzinger, S. Link between Isoprene and Secondary Organic Aerosol (SOA): Pyruvic Acid Oxidation Yields Low Volatility Organic Acids in Clouds. *Geophys. Res. Lett.* **2006**, *33*, L06822.

(12) Ortiz-Montalvo, D. L.; Lim, Y. B.; Perri, M. J.; Seitzinger, S. P.; Turpin, B. J. Volatility and Yield of Glycolaldehyde SOA Formed through Aqueous Photochemistry and Droplet Evaporation. *Aerosol Sci. Technol.* **2012**, *46*, 1002−1014.
(13) Reed Harris, A. E.; Ervens, B.; Shoemaker, R. K.; Rapf, R. J.; Kroll, J. A.; Griffith, E. C.; Monod, A.; Vaida, V. Photochemical Kinetics of Pyruvic Acid in Aqueous Solution. *J. Phys. Chem. A* **2014**, *118*, 8505−8516.
(14) Renard, P.; Siekmann, F.; Salque, G.; Smaani, A.; Demelas, C.; Coulomb, B.; Vassalo, L.; Ravier, S.; Temime-Roussel, B.; Voisin, D.; et al. Aqueous Phase Oligomerization of Methyl Vinyl Ketone through Photooxidation − Part 1: Aging Processes of Oligomers. *Atmos. Chem. Phys. Discuss.* **2014**, *14*, 15283−15322.
(15) Griffith, E. C.; Carpenter, B. K.; Shoemaker, R. K.; Vaida, V. Photochemistry of Aqueous Pyruvic Acid. *Proc. Natl. Acad. Sci. U.S.A.* **2013**, *110*, 11714−11719.
(16) Finlayson-Pitts, B. J.; Pitts, J. N. *Chemistry of the Upper and Lower Atmosphere: Theory, Experiment, and Applications*; Academic Press: San Diego, 2000; Chapter 9.
(17) Sorjamaa, R.; Svenningsson, B.; Raatikainen, T.; Henning, S.; Bilde, M.; Laaksonen, A. The Role of Surfactants in Köhler Theory Reconsidered. *Atmos. Chem. Phys.* **2004**, *4*, 2107−2117.
(18) Charlson, R. J.; Seinfeld, J. H.; Nenes, A.; Kulmala, M.; Laaksonen, A.; Facchini, M. C. Reshaping the Theory of Cloud Formation. *Science* **2001**, *292*, 2025−2026.
(19) Ellison, G. B.; Tuck, A. F.; Vaida, V. Atmospheric Processing of Organic Aerosols. *J. Geophys. Res.* **1999**, *104*, 633−641.
(20) Donaldson, D. J.; Vaida, V. The Influence of Organic Films at the Air-Aqueous Boundary on Atmospheric Processes. *Chem. Rev.* **2006**, *106*, 1445−1461.
(21) Guenther, A.; Karl, T.; Harley, P.; Wiedinmyer, C.; Palmer, P. I.; Geron, C. Estimates of global terrestrial isoprene emissions using MEGAN (Model of Emissions of Gases and Aerosols from Nature). *Atmos. Chem. Phys.* **2006**, *6*, 3181−3210.
(22) Lee, W.; Baasandorj, M.; Stevens, P. S.; Hites, R. A. Monitoring OH-Initiated Oxidation Kinetics of Isoprene and Its Products Using Online Mass Spectrometry. *Environ. Sci. Technol.* **2005**, *39*, 1030−1036.
(23) Kroll, J. H.; Ng, N. L.; Murphy, S. M.; Flagan, R. C.; Seinfeld, J. H. Secondary Organic Aerosol Formation from Isoprene Photooxidation. *Environ. Sci. Technol.* **2006**, *40*, 1869−1877.
(24) Dommen, J.; Metzger, A.; Duplissy, J.; Kalberer, M.; Alfarra, M. R.; Gascho, A.; Weingartner, E.; Prevot, A. S. H.; Verheggen, B.; Baltensperger, U. Laboratory Observation of Oligomers in the Aerosol from Isoprene/NOx Photooxidation. *Geophys. Res. Lett.* **2006**, *33*, L13805.
(25) Surratt, J. D.; Murphy, S. M.; Kroll, J. H.; Ng, N. L.; Hildebrandt, L.; Sorooshian, A.; Szmigielski, R.; Vermeylen, R.; Maenhaut, W.; Claeys, M.; et al. Chemical Composition of Secondary Organic Aerosol Formed from the Photooxidation of Isoprene. *J. Phys. Chem. A* **2006**, *110*, 9665−9690.
(26) Altieri, K. E.; Carlton, A. G.; Lim, H.-J.; Turpin, B. J.; Seitzinger, S. P. Evidence for Oligomer Formation in Clouds: Reactions of Isoprene Oxidation Products. *Environ. Sci. Technol.* **2006**, *40*, 4956−4960.
(27) Altieri, K. E.; Seitzinger, S. P.; Carlton, A. G.; Turpin, B. J.; Klein, G. C.; Marshall, A. G. Oligomers Formed Through in-Cloud Methylglyoxal Reactions: Chemical Composition, Properties, and Mechanisms Investigated by Ultra-High Resolution FT-ICR Mass Spectrometry. *Atmos. Environ.* **2008**, *42*, 1476−1490.
(28) Perri, M.; Seitzinger, S. P.; Turpin, B. J. Secondary Organic Aerosol Production from Aqueous Photooxidation of Glycolaldehyde: Laboratory Experiments. *Atmos. Environ.* **2009**, *43*, 1487−1497.
(29) El Haddad, I.; Liu, Y.; Nieto-Gligorovski, L.; Michaud, V.; Temime-Roussel, B.; Quivet, E.; Marchand, N.; Sellegri, K.; Monod, A. In-Cloud Processes of Methacrolein under Simulated Conditions - Part 2: Formation of Secondary Organic Aerosol. *Atmos. Chem. Phys.* **2009**, *9*, 5107−5117.
(30) Tan, Y.; Perri, M. J.; Seitzinger, S. P.; Turpin, B. J. Effects of Precursor Concentration and Acidic Sulfate in Aqueous Glyoxal-OH Radical Oxidation and Implications for Secondary Organic Aerosol. *Environ. Sci. Technol.* **2009**, *43*, 8105−8112.
(31) Tan, Y.; Carlton, A. G.; Seitzinger, S. P.; Turpin, B. J. SOA from Methylglyoxal in Clouds and Wet Aerosols: Measurement and Prediction of Key Products. *Atmos. Environ.* **2010**, *44*, 5218−5226.
(32) Lim, Y. B.; Tan, Y.; Turpin, B. J. Chemical Insights, Explicit Chemistry, and Yields of Secondary Organic Aerosol from OH Radical Oxidation of Methylglyoxal and Glyoxal in the Aqueous Phase. *Atmos. Chem. Phys.* **2013**, *13*, 8651−8667.
(33) Donaldson, D. J.; Valsaraj, K. T. Adsorption and Reaction of Trace Gas-Phase Organic Compounds on Atmospheric Water Film Surfaces: A Critical Review. *Environ. Sci. Technol.* **2010**, *44*, 865−873.
(34) Zhang, X.; Chen, Z. M.; Zhao, Y. Laboratory Simulation for the Aqueous OH-Oxidation of Methyl Vinyl Ketone and Methacrolein: Significance to the in-Cloud SOA Production. *Atmos. Chem. Phys.* **2010**, *10*, 9551−9561.
(35) Liu, Y.; Siekmann, F.; Renard, P.; El Zein, A.; Salque, G.; El Haddad, I.; Temime-Roussel, B.; Voisin, D.; Thissen, R.; Monod, A. Oligomer and SOA Formation through Aqueous Phase Photooxidation of Methacrolein and Methyl Vinyl Ketone. *Atmos. Environ.* **2012**, *49*, 123−129.
(36) Chan, K. M.; Huang, D. D.; Li, Y. J.; Chan, M. N.; Seinfeld, J. H.; Chan, C. K. Oligomeric Products and Formation Mechanisms from Acid-Catalyzed Reactions of Methyl Vinyl Ketone on Acidic Sulfate Particles. *J. Atmos. Chem.* **2013**, *70*, 1−18.
(37) Schöne, L.; Schindelka, J.; Szeremeta, E.; Schaefer, T.; Hoffmann, D.; Rudzinski, K. J.; Szmigielski, R.; Herrmann, H. Atmospheric Aqueous Phase Radical Chemistry of the Isoprene Oxidation Products Methacrolein, Methyl Vinyl Ketone, Methacrylic Acid and Acrylic Acid - Kinetics and Product Studies. *Phys. Chem. Chem. Phys.* **2014**, *16*, 6257−6272.
(38) Epstein, S. A.; Tapavicza, E.; Furche, F.; Nizkorodov, S. A. Direct Photolysis of Carbonyl Compounds Dissolved in Cloud and Fog Droplets. *Atmos. Chem. Phys.* **2013**, *13*, 9461−9477.
(39) Vesley, G. F.; Leermakers, P. A. Photochemistry of α-Keto Acids and α-Keto Esters. 3. Photolysis of Pyruvic Acid in Vapor Phase. *J. Phys. Chem.* **1964**, *68*, 2364−2366.
(40) Yamamoto, S.; Back, R. A. The Photolysis and Thermal Decomposition of Pyruvic Acid in the Gas Phase. *Can. J. Chem.* **1985**, *63*, 549−554.
(41) Mellouki, A.; Mu, Y. J. On the Atmospheric Degradation of Pyruvic Acid in the Gas Phase. *J. Photochem. Photobiol., A* **2003**, *157*, 295−300.
(42) Closs, G. L.; Miller, R. J. Photo-Reduction and Photodecarbosylation of Pyruvic Acid-Applications of CIDNP to Mechanistic Photochemistry. *J. Am. Chem. Soc.* **1978**, *100*, 3483−3494.
(43) Leermakers, P. A.; Vesley, G. F. Photochemistry of α-Keto Acids and α-Keto-Esters. 1. Photolysis of Pyruvic Acid and Benzoylformic Acid. *J. Am. Chem. Soc.* **1963**, *85*, 3776−3779.
(44) Leermakers, P. A.; Vesley, G. F. Photolysis of Pyruvic Acid in Solution. *J. Org. Chem.* **1963**, *28*, 1160−1161.
(45) Guzman, M. I.; Colussi, A. J.; Hoffmann, M. R. Photoinduced Oligomerization of Aqueous Pyruvic Acid. *J. Phys. Chem. A* **2006**, *110*, 3619−3626.
(46) Takahashi, K.; Plath, K. L.; Skodje, R. T.; Vaida, V. Dynamics of Vibrational Overtone Excited Pyruvic Acid in the Gas Phase: Line Broadening through Hydrogen-Atom Chattering. *J. Phys. Chem. A* **2008**, *112*, 7321−7331.
(47) Plath, K. L.; Takahashi, K.; Skodje, R. T.; Vaida, V. Fundamental and Overtone Vibrational Spectra of Gas-Phase Pyruvic Acid. *J. Phys. Chem. A* **2009**, *113*, 7294−7303.
(48) Larsen, M. C.; Vaida, V. Near Infrared Photochemistry of Pyruvic Acid in Aqueous Solution. *J. Phys. Chem. A* **2012**, *116*, 5840−5846.
(49) Ervens, B.; Wang, Y.; Eagar, J.; Leaitch, W. R.; Macdonald, A. M.; Valsaraj, K. T.; Herckes, P. Dissolved Organic Carbon (DOC) and Select Aldehydes in Cloud and Fog Water: the Role of the Aqueous

Phase in Impacting Trace Gas Budgets. *Atmos. Chem. Phys.* **2013**, *13*, 5117−5135.
(50) Kameel, F.; Hoffmann, M. R.; Colussi, A. J. OH Radical-Initiated Chemistry of Isoprene in Aqueous Media. Atmospheric Implications. *J. Phys. Chem. A* **2013**, *117*, 5117−5123.
(51) Bao, L.; Matsumoto, M.; Kubota, T.; Sekiguchi, K.; Wang, Q.; Sakamoto, K. Gas/Particle Partitioning of Low-Molecular-Weight Dicarboxylic Acids at a Suburban Site in Saitama, Japan. *Atmos. Environ.* **2012**, *47*, 546−553.
(52) Herrmann, H.; Hoffmann, D.; Schaefer, T.; Bräuer, P.; Tilgner, A. Tropospheric Aqueous-Phase Free-Radical Chemistry: Radical Sources, Spectra Reaction Kinetics and Prediction Tools. *Chem. Phys. Chem.* **2010**, *11*, 3796−3822.
(53) Ervens, B.; Volkamer, R. Glyoxal Processing by Aerosol Multiphase Chemistry: Towards a Kinetic Modeling Framework of Secondary Organic Aerosol Formation in Aqueous Particles. *Atmos. Chem. Phys.* **2010**, *10*, 8219−8244.
(54) Arakaki, T.; Anastasio, C.; Kuroki, Y.; Nakajima, H.; Okada, K.; Kotani, Y.; Handa, D.; Azechi, S.; Kimura, T.; Tsuhako, A.; Miyagi, Y. A General Scavenging Rate Constant for Reaction of Hydroxyl Radical with Organic Carbon in Atmospheric Waters. *Environ. Sci. Technol.* **2013**, *47*, 8196−8203.
(55) Griffith, E. C.; Adams, E. M.; Allen, H. C.; Vaida, V. Hydrophobic Collapse of a Stearic Acid Film by Adsorbed L-Phenylalanine at the Air−Water Interface. *J. Phys. Chem. B* **2012**, *116*, 7849−7857.
(56) Adamson, A. W.; Gast, A. P. *Physical Chemistry of Surfaces*; John Wiley and Sons, Inc.: New York, 1997.
(57) Maroń, M. K.; Takahashi, K.; Shoemaker, R. K.; Vaida, V. Hydration of Pyruvic Acid to its Geminal-Diol, 2,2-Dihydroxypropanoic Acid, in a Water-Restricted Environment. *Chem. Phys. Lett.* **2011**, *513*, 184−190.
(58) Griffith, E. C.; Shoemaker, R. K.; Vaida, V. Sunlight-initiated Chemistry of Aqueous Pyruvic Acid: Building Complexity in the Origin of Life. *Origins Life Evol. Biospheres* **2013**, *43*, 341−352.
(59) Gibian, M. J.; Corley, R. C. Organic Radical-Radical Reactions. Disproportionation vs Combination. *Chem. Rev.* **1973**, *73*, 441−464.
(60) Ervens, B.; Sorooshian, A.; Lim, Y. B.; Turpin, B. J. Key Parameters Controlling OH-Initiated Formation of Secondary Organic Aerosol in the Aqueous Phase (aqSOA). *J. Geophys. Res. Atmos.* **2014**, *119*, 3997−4016.
(61) Decker, C.; Jenkins, A. D. Kinetic Approach of O_2 Inhibition in Ultraviolet- and Laser-Induced Polymerizations. *Macromolecules* **1985**, *18*, 1241−1244.
(62) Odian, G. *Principles of Polymerization*; John Wiley and Sons, Inc.: Hoboken, NJ, 2004.
(63) Ligon, S. C.; Husár, B.; Wutzel, H.; Holman, R.; Liska, R. Strategies to Reduce Oxygen Inhibition in Photoinduced Polymerization. *Chem. Rev.* **2014**, *114*, 557−589.
(64) Kameel, F. R.; Riboni, F.; Hoffmann, M. R.; Enami, S.; Colussi, A. J. Fenton Oxidation of Gaseous Isoprene on Aqueous Surfaces. *J. Phys. Chem. C* **2014**, DOI: 10.1021/jp505010e.
(65) Dobson, C. M.; Ellison, G. B.; Tuck, A. F.; Vaida, V. Atmospheric Aerosols as Prebiotic Chemical Reactors. *Proc. Natl. Acad. Sci. U.S.A.* **2000**, *97*, 11864−11868.
(66) Gill, P. S.; Graedel, T. E.; Weschler, C. J. Organic Films on Atmospheric Aerosol Particles, Fog Droplets, Cloud Droplets, Raindrops, and Snowflakes. *Rev. Geophys. Space Phys.* **1983**, *21*, 903−920.
(67) Rudich, Y.; Abo, R. A.; Erlick, C.; Adler, G.; Trainic, M.; Lang, N. Optical Properties of Aerosols with Organic Components Using Cavity Ring Down Spectrometry. *Geochim. Cosmochim.* **2009**, A1130−A1130.
(68) Kaku, K. C.; Hegg, D. A.; Covert, D. S.; Santarpia, J. L.; Jonsson, H.; Buzorius, G.; Collins, D. R. Organics in the Northeastern Pacific and their Impacts on Aerosol Hygroscopicity in the Subsaturated and Supersaturated Regimes. *Atmos. Chem. Phys.* **2006**, *6*, 4101−4115.
(69) Gilman, J. B.; Tervahattu, H.; Vaida, V. Interfacial Properties of Mixed Films of Long Chain Organics at the Air−Water Interface. *Atmos. Environ.* **2006**, *40*, 6606−6614.
(70) Prather, K. A.; et al. Ocean Impacts on Sea Spray Aerosol Chemistry and Climate. *Proc. Natl. Acad. Sci. U.S.A.* **2013**, *110*, 7550−7555.
(71) McNeill, V. F.; Sareen, N.; Schwier, A. N. Surface Active Organic in Atmospheric Aerosols. *Top. Curr. Chem.* **2014**, *339*, 201−259.
(72) Tervahattu, H.; Hartonen, K.; Kerminen, V.-M.; Kupiainen, K.; Aarnio, P.; Koskentalo, T.; Tuck, A. F.; Vaida, V. New Evidence of an Organic Layer on Marine Aerosols. *J. Geophys. Res.: Atmos.* **2002a**, *107*, AAC 1−1−AAC 1−8.
(73) Tervahattu, H.; Juhanoja, J.; Kupiainen, K. J. Identification of an Organic Coating on Marine Aerosol Particles by TOF-SIMS. *J. Geophys. Res.: Atmos.* **2002b**, *107*, ACH 18−1−ACH 18−7.
(74) Tervahattu, T.; Juhanoja, J.; Vaida, V.; Tuck, A. F.; Niemi, J. V.; Kupiainen, K.; Kulmala, M.; Vehkamäki, H. Fatty Acids on Continental Sulfate Aerosol Particles. *J. Geophys. Res.* **2005**, *110*, 207.
(75) Prather, K. A.; Hatch, C. D.; Grassian, V. H. Analysis of Atmospheric Aerosols. *Annu. Rev. Anal. Chem. (Palo Alto, Calif)* **2008**, *1*, 485−514.
(76) Barnes, G. T. The Effects of Monolayers on the Evaporation of Liquids. *Adv. Colloid Interface Sci.* **1986**, *25*, 89−200.
(77) Gilman, J. B.; Vaida, V. Permeability of Acetic Acid through Organic Films at the Air-Aqueous Interface. *J. Phys. Chem. A* **2006**, *110*, 7581−7587.
(78) Mmereki, B. T.; Chaudhuri, S. R.; Donaldson, D. J. Enhanced Uptake of PAHs by Organic-Coated Aqueous Surfaces. *J. Phys. Chem. A* **2003**, *107*, 2264−2269.
(79) Mmereki, B. T.; Donaldson, D. J. Direct Observation of the Kinetics of an Atmospherically Important Reaction at the Air−Aqueous Interface. *J. Phys. Chem. A* **2003**, *107*, 11038−11042.
(80) Davies, J. F.; Miles, R. E. H.; Haddrell, A. E.; Reid, J. P. Influence of Organic Films on the Evaporation and Condensation of Water in Aerosol. *Proc. Natl. Acad. Sci. U.S.A.* **2013**, *110*, 8807−8812.
(81) Park, S. C.; Burden, D. K.; Nathanson, G. M. Surfactant Control of Gas Transport and Reactions at the Surface of Sulfuric Acid. *Acc. Chem. Res.* **2009**, *42*, 379−387.
(82) Lo, J.-H. A.; Lee, W.-M. G. Effect of Surfactant Film on Solubility of Hydrophobic Organic Compounds in Fog Droplets. *Chemosphere* **1996**, *33*, 1391−1408.
(83) Bertram, A. K.; Ivanov, A. V.; Hunter, M.; Molina, L. T.; Molina, M. J. The Reaction Probability of OH on Organic Surfaces of Tropospheric Interest. *J. Phys. Chem. A* **2001**, *105*, 9415−9421.
(84) Eliason, T. L.; Gilman, J. B.; Vaida, V. Oxidation of Organic Films Relevant to Atmospheric Aerosols. *Atmos. Environ.* **2004**, *38*, 1367−1378.
(85) Mmereki, B. T.; Donaldson, D. J.; Gilman, J. B.; Eliason, T. L.; Vaida, V. Kinetics and Products of the Reaction of Gas-Phase Ozone with Anthracene Adsorbed at the Air−Aqueous Interface. *Atmos. Environ.* **2004**, *38*, 6091−6103.
(86) Rudich, Y. Laboratory Perspectives on the Chemical Transformations of Organic Matter in Atmospheric Particles. *Chem. Rev.* **2003**, *103*, 5097−5124.
(87) Rudich, Y.; Donahue, N. M.; Mentel, T. F. Aging of Organic Aerosol: Bridging the Gap between Laboratory and Field Studies. *Annu. Rev. Phys. Chem.* **2007**, *58*, 321−352.
(88) Wadia, Y.; Tobias, D. J.; Stafford, R.; Finlayson-Pitts, B. J. Real-Time Monitoring of the Kinetics and Gas-Phase Products of the Reaction of Ozone with an Unsaturated Phospholipid at the Air−Water Interface. *Langmuir* **2000**, *16*, 9321−9330.
(89) Chakraborty, P.; Zachariah, M. R. On the Structure of Organic-Coated Water Droplets: From "Net Water Attractors" to "Oily" Drops. *J. Geophys. Res.: Atmos.* **2011**, *116*, D21205.
(90) Clifford, D.; Bartels-Rausch, T.; Donaldson, D. J. Suppression of Aqueous Surface Hydrolysis by Monolayers of Short Chain Organic Amphiphiles. *Phys. Chem. Chem. Phys.* **2007**, *9*, 1362−1369.

(91) Blower, P. G.; Shamay, E.; Kringle, L.; Ota, S. T.; Richmond, G. L. Surface Behavior of Malonic Acid Adsorption at the Air/Water Interface. *J. Phys. Chem. A* **2013**, *117*, 2529−2542.
(92) Li, Y.; Ezell, M. J.; Finlayson-Pitts, B. J. The Impact of Organic Coatings on Light Scattering by Sodium Chloride Particles. *Atmos. Environ.* **2011**, *45*, 4123−4132.